9th International Conference on Photonic Technologies - LANE 2016

Influence of process parameters on the quality of aluminium alloy EN AW 7075 using selective laser melting (SLM)

Kaufmann, N.[a],[*], Imran, M.[b], Wischeropp, T. M.[a], Emmelmann, C.[a],[c], Siddique, S.[b], Walther, F.[b]

[a]Institut of Laser and System Technologies (iLAS), Hamburg University of Technology (TUHH), Denickestr. 17, 21073 Hamburg, Germany
[b]Department of Materials Test Engineering (WPT), TU Dortmund University, Baroper Str. 303, 44227 Dortmund, Germany
[c]LZN Laser Zentrum Nord GmbH, Am Schleusengraben 14, 21029 Hamburg, Germany

Abstract

Selective laser melting (SLM) is an additive manufacturing process, forming the desired geometry by selective layer fusion of powder material. Unlike conventional manufacturing processes, highly complex parts can be manufactured with high accuracy and little post processing. Currently, different steel, aluminium, titanium and nickel-based alloys have been successfully processed; however, high strength aluminium alloy EN AW 7075 has not been processed with satisfying quality. The main focus of the investigation is to develop the SLM process for the wide used aluminium alloy EN AW 7075. Before process development, the gas-atomized powder material was characterized in terms of statistical distribution: size and shape. A wide range of process parameters were selected to optimize the process in terms of optimum volume density. The investigations resulted in a relative density of over 99 %. However, all laser-melted parts exhibit hot cracks which typically appear in aluminium alloy EN AW 7075 during the welding process. Furthermore the influence of processing parameters on the chemical composition of the selected alloy was determined.

Keywords: EN AW 7075; aluminium alloy; hot cracks; relative density; selective laser melting (SLM)

* Corresponding author: +49-40-484010-727 ; fax: +49-40-484010-999 .
 E-mail address: n.kaufmann@tuhh.de

1. Introduction

Selective laser melting (SLM) is an additive manufacturing process with a high potential for manufacturing of high quality metal parts. A 3-dimensional CAD design is sliced into 2-dimension slices with a layer thickness which is equivalent to the layer thickness during the SLM process (typically 30-100 µm). The powder bed layer is locally scanned and melted by a laser. In this way the parts are produced layer-by-layer.

The buildup rate $\dot{v}$ [mm³/s] is one of the important characteristics to compare the productivity of the SLM process. The calculation of the volume buildup rate for the primary processing time is the function of layer thickness D_s [mm], scanning speed v_s [mm/s] and hatch distance h_s [mm] [1]:

$$\dot{v} = D_S \cdot v_S \cdot h_S \tag{1}$$

Another important characteristic of the process is the volume energy E_v [J/mm³]. It is calculated by dividing the laser power P_L [W] by the buildup rate $\dot{v}$ [mm³/s] [2]:

$$E_V = \frac{P_L}{\dot{v}} \tag{2}$$

The high-strength aluminium alloy EN AW 7075, also known as AlZn5.5MgCu or AlZnMgCu1.5, has a high tensile strength of over 500 MPa in comparison to other aluminium alloys [3]. Furthermore, AN EW 7075 exhibits a high corrosion resistance. Alloys of aluminium 7XXX series are known to have very good fatigue properties in comparison to other aluminium alloys [4] [5].

One of the major disadvantages of EN AW 7075 is the high sensitivity to hot cracks during rapid solidification and therefore poor weldability. Hot cracks appear inter-crystalline during the solidification between the solidus and liquidus temperature. During solidification, the viscosity of the melting phase increases and therefore the melt cannot flow contrary to direction of consolidation to fill the voidage between grains caused by shrinkage [6]. In order to prevent hot cracks, a preheating temperature has shown a positive effect [7].

2. Powder characteristics

The powder EN AW 7075 was inert gas-atomized and the desired particle size ranges between 20 µm and 63 µm.

2.1. Apparent density

The apparent density was measured in accordance with DIN EN ISO 3923-1 [8]. The apparent density $\rho_{Apparent}$ is 1.19 g/cm³. Furthermore, the packing factor k is calculated by using the equation (3) [9]. The density of solid material ρ_{Solid} of EN AW 7075 is 2.80 g/cm³. The result of the packing factor is $k = 42.5$ %.

$$k = \frac{\rho_{Apparent}}{\rho_{Solid}} \cdot 100\% \tag{3}$$

2.2. Particle morphology

The particle morphology was determined by using the Scanning Electron Microscope (SEM) *Leo Gemini 1530*. The particles were spread on an adhesive electrically conductive plate. Figure 1 illustrates that the majority of particles are elliptical.
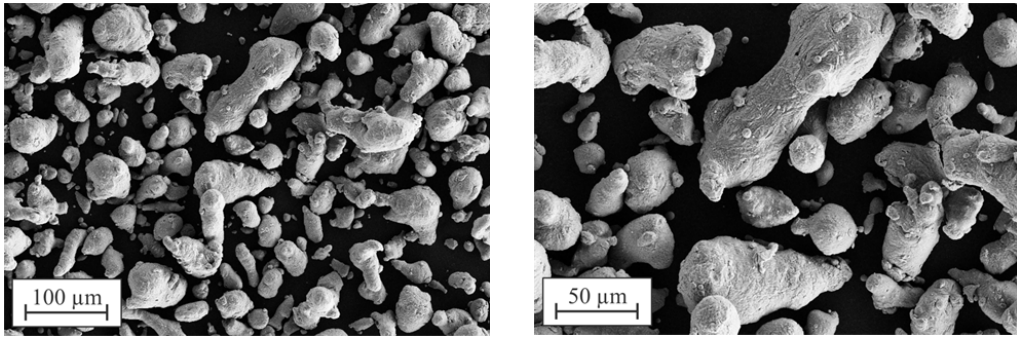
Fig. 1. SEM images of powder material EN AW 7075, overview (left) and detail (right).

2.3. Particle size distribution

The particle size distribution was measured in accordance with ISO 13320 using a *Beckman Coulter LS13320* laser diffractometer [10]. Figure 2 shows the cumulative frequency and the distribution density. Approximately 30 % of particle volume is higher than maximum desired particle size of 63 µm and 5 % of particle volume is lower than minimum desired particle size of 20 µm.

One possible explanation for this is the elliptical shape of the particles. Although the equivalent diameter is larger than the mesh size, they can pass through the sieve if their longitudinal axis is perpendicular to the sieve [9].
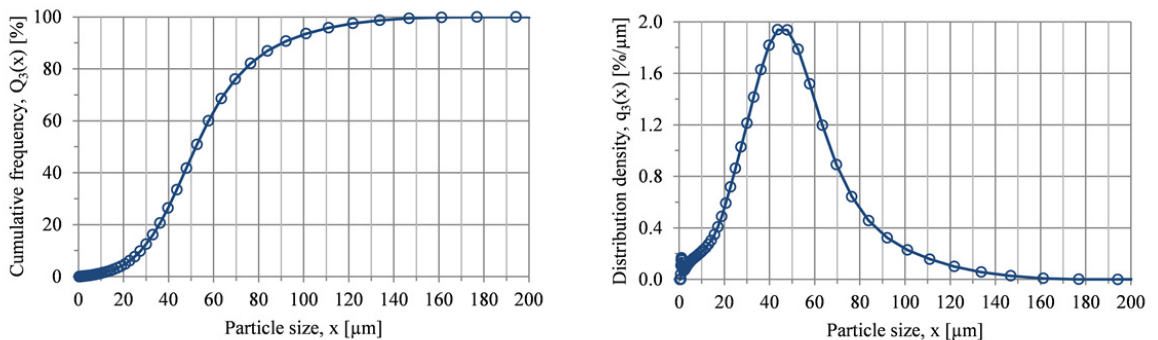

Fig. 2. Cumulative frequency $Q_3(x)$ (left) and distribution density $q_3(x)$ (right).

2.4. Chemical composition

Table 1 shows the chemical composition of the EN AW 7075 powder compared to DIN EN 573-3:2013-12 [11]. During the manufacturing process of the powder material, Inert Gas Fusion (IGF) method was used to measure the oxygen and Inductively Coupled Plasma and Optical Emission Spectroscopy (ICP-OES) method to determine the rest of the elements. The chemical composition of powder material used is in agreement with DIN EN 573-3:2013-12.

Table 1. Chemical composition of EN AW 7075.

Element	DIN EN 573-3:2013-12 (min – max) [wt%] [11]	as-delivered [wt%]
Cr	0.18 – 0.28	0.20
Cu	1.2 – 2.0	1.3
Fe	0.00 – 0.50	0.12
Mg	2.1 – 2.9	2.2
Mn	0.00 – 0.30	< 0.01
O	–	0.08
Si	0.00 – 0.40	0.07
Ti	0.00 – 0.20	< 0.01
Zn	5.1 – 6.1	5.2
Other	0.00 – 0.05	0.01
All Others	0.00 – 0.15	< 0.10
Al	remaining	remaining

3. Specimens manufacturing

3.1. Process parameters and system

For the manufacturing of specimens, SLM 250-HL system, equipped with a ROFIN FL 010 S 1 kW laser, was used. For the specimens, a layer thickness (D_s) of 0.05 mm and a hatch distance (h_s) of 0.13 mm was used. The laser power was varied in the range of 100 to 600 W and scanning speed between 250 and 2000 mm/s. The specimens were manufactured at different base plate heating temperatures of 40 and 200 °C.

Before starting the SLM 250 HL machine the building chamber was filled with argon gas to reduce oxygen. Each building job was started with an oxygen value lower than 0.05 %.

3.2. Geometry of specimens

Figure 3 shows the geometry of the laser-melted test specimen, which is a combination of a cube and a pyramid and is used for density measurement. The pyramid structure was used for easy removal from the base plate. The height of the entire specimen is about 15 mm and the dimension of the cube is 10 x 10 x 10 mm³.
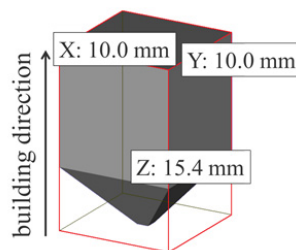

Fig. 3. Specimen geometry for density measurement.

4. Results and discussions

4.1. Relative density

The relative density of the laser-melted specimens was optically measured [12] with Olympus *GX51* microscope. Each specimen was cut and polished parallel to the build direction. Figure 4 shows an image of polished specimen and the chosen region of interest (ROI) for relative density measurement. The red spots indicate the porosity.
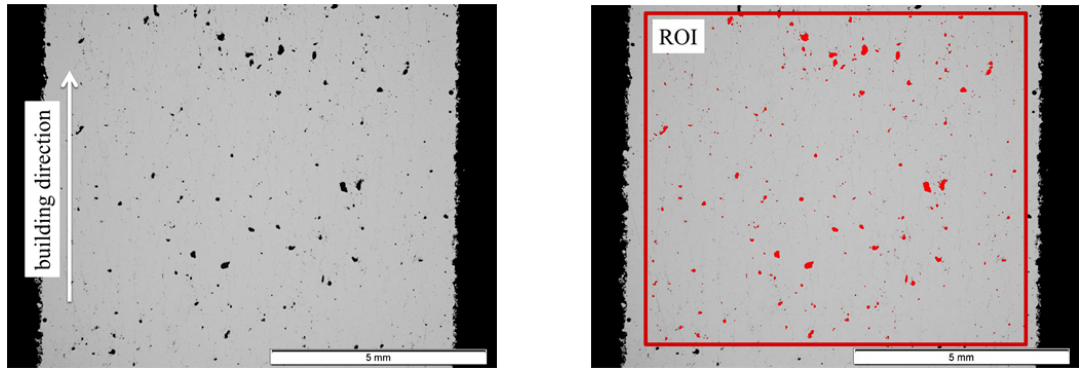

Fig. 4. Image of a polished specimen (left) and region of interest - ROI (right).

Figure 5 exemplarily shows the relative density of selected specimens depending on different values of scanning speed v_s and laser power P_L. The higher the laser power in combination with lower scanning speed, the higher is the relative density of the specimens.
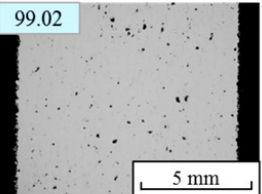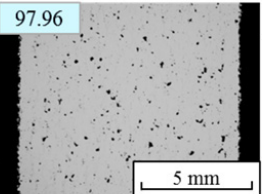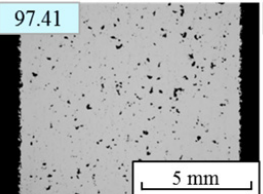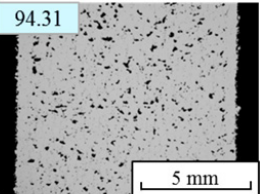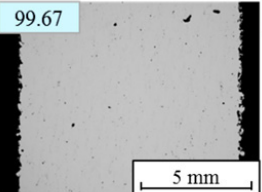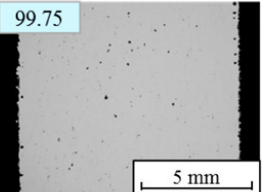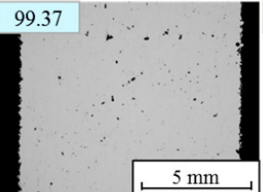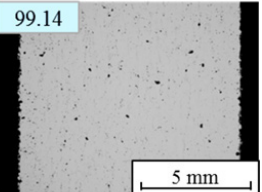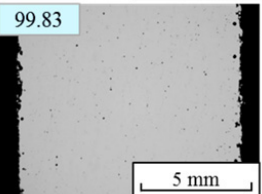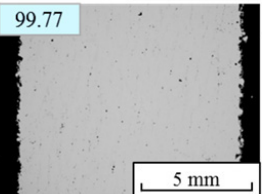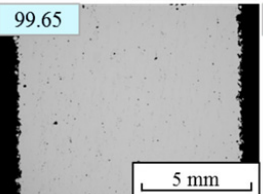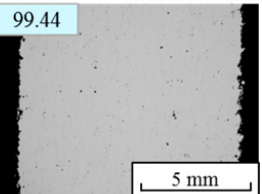

Fig. 5. Image of polished specimens, relative density (top left of images) plotted against scanning speed and laser power.

In Figure 6 the relative density is plotted against scanning speed for five different values of laser power. On the one hand the relative density decreases with increasing scanning speed at constant laser power. On the other hand the relative density augmented with increasing laser power at constant scanning speed. With increasing laser power and scanning speed, it is possible to get buildup rate higher than 13.0 mm³/s with a relative density over 99 %. With a laser power of 300 W and scanning speed of 1200 mm/s, the volume buildup rate of 7.8 mm³/s can be achieved. With a laser power of 500 W and scanning speed of 2000 mm/s it is possible to get a buildup rate higher than 13.0 mm³/s.
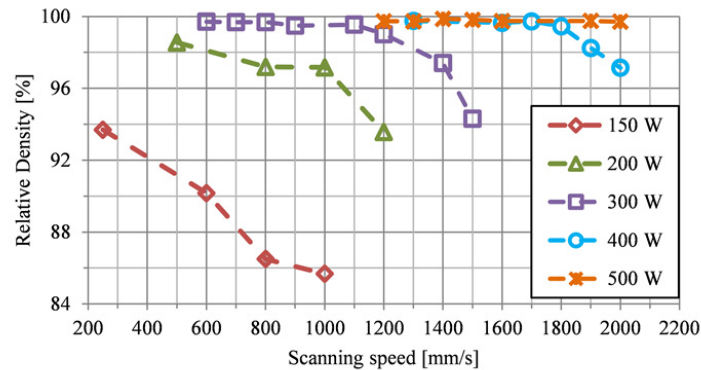

Fig. 6. Density curves plotted against scanning speed regarded to five different values of laser power.

In Figure 7 the relative density is plotted against laser power for three different values of volume energy. With constant volume energy, the relative density enhances by increasing the laser power. In order to keep the volume energy constant, the scanning speed was varied in the same proportion as the laser power. In order to increase the relative density, a relatively high laser power is required as shown in Figure 6.
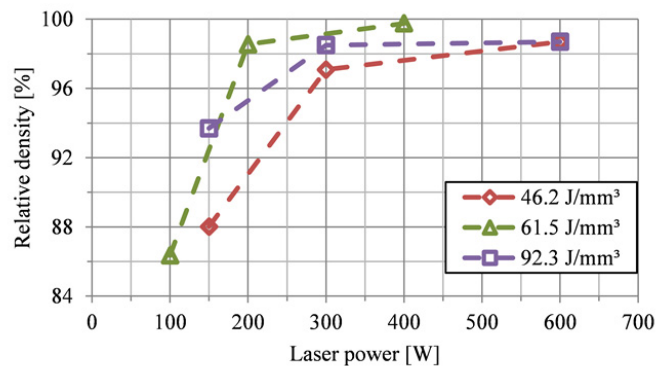
Fig. 7. Relative density curves plotted against laser power for three different values of volume energy.

4.2. Chemical composition

The chemical composition for the laser-melted specimen was measured with SEM-EDX by using Tescan *Mira XMU* (EOS). Due to different measuring methods it may come to differences in the chemical composition of the powder, which was determined with ICP-OES and IGF, and the laser-melted specimen. The investigated specimen was manufactured with the laser power of 500 W and the scanning speed of 1500 mm/s. In Table 2, the chemical composition for the powder material and manufactured specimen is compared. For other process parameters the chemical composition for laser melted specimen may be different. The results show that the percentage of

chromium, copper, steel, manganese, oxygen, silicon and titanium increased. The value of silicon is out of allowable range defined in DIN EN 573-3:2013-12.

The major problem in manufacturing of the specimen is expected due to the fact that the value of zinc decreases over 1.6 wt%. One of the conceivable reasons is that zinc is vaporizing during the SLM process. The evaporation temperature of zinc with 907 °C is much lower than the evaporation temperature of aluminium with 2519 °C.

Table 2. Chemical composition of EN AW 7075.

Element	DIN EN 573-3:2013-12 (min – max) [wt%] [11]	powder [wt%]	laser-melted specimen [wt%]
Cr	0.18 – 0.28	0.20	0.25
Cu	1.2 – 2.0	1.3	1.61
Fe	0.00 – 0.50	0.12	0.19
Mg	2.1 – 2.9	2.2	2.2
Mn	0.00 – 0.30	< 0.01	0.08
O	–	0.08	2.08
Si	0.00 – 0.40	0.07	0.47
Ti	0.00 – 0.20	< 0.01	0.08
Zn	5.1 – 6.1	5.2	3.6
Al	remaining	remaining	remaining

4.3. Hot cracks

Hot cracks occur in all laser-melted specimens in line with expectations (see chapter 1). In Figure 8 the hot cracks are exemplary marked. The major progression of the hot cracks is in building direction.

During the SLM process residual stresses in manufactured parts are caused due to the temperature gradient parallel to building direction [15]. Therefore the residual stresses may amplify the progression of hot cracks in building direction. And the solidification occurs in building direction and this will also lead to hot cracks in that direction.
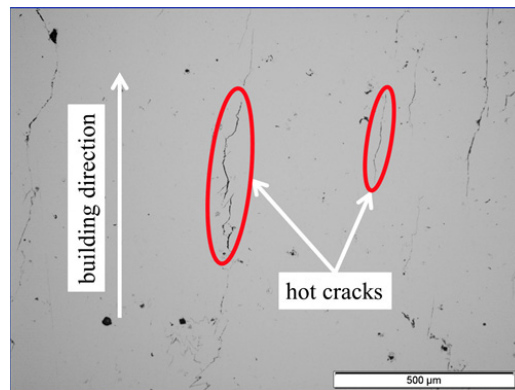

Fig. 8. Exemplary hot cracks in laser-melted test specimen (base plate temperature: 200 °C, v_s = 1200 mm/s, P_L = 500 W).

In order to investigate the trend of hot cracks due to the variation of the preheating temperature for the base plate, two different values were chosen. All the other process parameters were set constant. In Figure 9, the effect of the preheating temperature: 40 °C (left) and 200 °C (right), is shown. There was no significant influence observed on hot cracks by variation of preheating temperature for all specimens. One assumption is that the preheating temperature of 200 °C was not high enough to significantly reduce hot cracks.
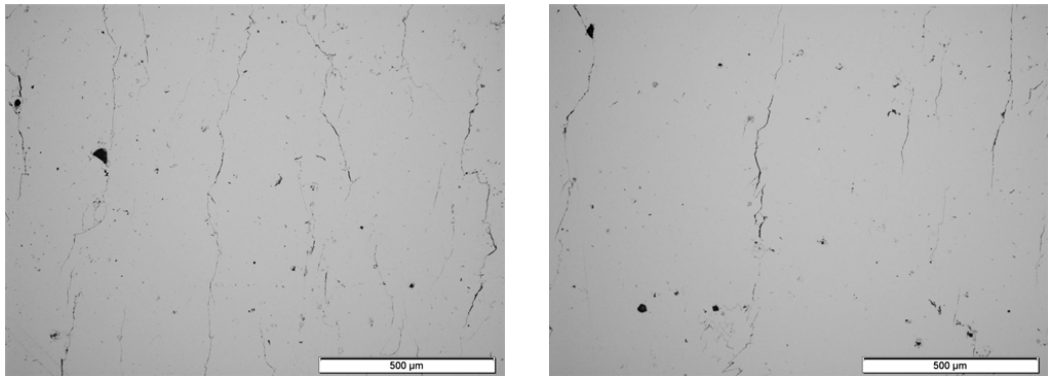
Fig. 9. Hot cracks: preheating temperature of 40 °C (left) and 200 °C (right).

The appearance of hot cracks is also increased by high cooling rates which are typical for the high thermal conductivity of aluminium [13]. Furthermore the hot cracks can be easily initiated by pores [14] due to obvious notch effect, Figure 10.
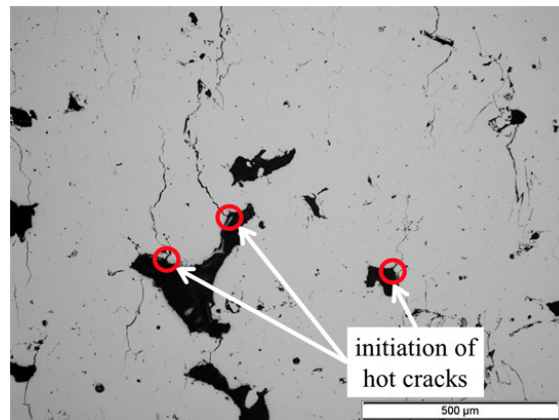

Fig. 10. Hot cracks, initiated by pores.

5. Conclusions and outlook

The aim of investigations presented in this paper was to discuss the processing potential and limitations of aluminium alloy EN AW 7075 by the selective laser melting.

The particle morphology and the particle size distribution were examined. The major particles are elliptical and therefore a wider range of the particle size distribution is observed. Elliptical particles with an equivalent diameter bigger than mesh size passed through the sieve.

A wide range of processing parameters has been tested. It was shown, that with high laser powers (> 300 W) high relative densities of over 99 % are possible. All investigated specimens showed progression of the hot cracks, with an orientation in building direction. A preheating temperature of up to 200 °C did not show a significant positive effect on reduction of hot cracks. From literature it is known that high cooling rates foster the origin of hot cracks. Therefore it will be investigated, if increasing layer thickness, preheating or re-melting with the laser, or working with bigger focus-size can reduce the amount of hot cracks. Furthermore, reducing the amount of hot cracks by hot isostatic pressuring is an option.

Additionally it was shown, that a significant amount of zinc is evaporated during the SLM process, due to low evaporation temperature of zinc in combination with high laser powers used. Therefore a trade-off between high densities on the one hand and change of chemical composition on the other hand will be necessary. A change of chemical composition of the powder material to compensate the evaporation of zinc is another option.

Acknowledgements

References

[1]   Buchbinder, D., Schleifenbaum, H., Heidrich, S., Meiners, W., Bültmann, J.: High Power Selective Laser Melting (HP SLM) of Aluminum Parts, In: Physics Procedia 12 (2011), 271–278.
[2]   Grund, M.: Implementierung von schichtadditiven Fertigungsverfahren - Mit Fallbeispielen aus der Luftfahrtindustrie und Medizintechnik, Springer, 2015.
[3]   Körner, C.: Aluminium Taschenbuch 1 - Grundlagen und Werkstoffe, 16. Aufl., 2012.
[4]   Boyer, H.E.: Atlas of fatigue curves. ASM international. 1986.
[5]   Wagner, L., Mhaede, M., Wollmann, M., Altenberger, I, Sano, Y.: Surface layer properties and fatigue behavior in Al 7075-T73 and Ti-6Al-4V: Comparing results after laser peening; shot peening and ball-burnishing, In: International Journal of Structural 2 (2011), 185–199.
[6]   Tang, Z.: Heißrissvermeidung beim Schweißen von Aluminiumlegierungen mit einem Scheibenlaser, BIAS, 2014.
[7]   Dilthey, U.: Schweißtechnische Fertigungsverfahren 2 - Verhalten der Werkstoffe beim Schweißen, Springer, 2005.
[8]   DIN EN ISO 3923-1: Metallic powders – Determination of apparent density – Part 1: Funnel method (ISO 3923-1:2008); German version EN ISO 3923-1, 2010.
[9]   Stieß, M.: Mechanische Verfahrenstechnik – Partikeltechnologie 1, Springer, 2009.
[10] ISO 13320: Particle size analysis - Laser diffraction methods, 2009.
[11] DIN EN 573-3: Aluminium and aluminium alloys – Chemical composition and form of wrought products – Part 3: Chemical composition and form of products; German version EN 573-3, 2013.
[12] VDI 3405: Additive manufacturing processes, rapid manufacturing beam melting of metallic parts - qualification, quality assurance and post processing, 2013.
[13] Fahrenwaldt, H. J., Schuler, V.: Praxiswissen Schweißtechnik - Werkstoffe, Prozesse, Fertigung, Vieweg & Sohn, 2006.
[14] Zhang, D.: Entwicklung des Selective Laser Melting (SLM) für Aluminiumwerkstoffe, Shaker, 2004.
[15] Munsch, M.: Reduzierung von Eigenspannungen und Verzug in der laseradditiven Fertigung, Cuvillier, 2013.